Flow and Heat Transfer Analysis of Williamson Viscous Fluid on the Stagnation Point past a Stretching Surface with Viscous Dissipation and Slip Conditions

Hasmawani Hashim[1], Muhammad Khairul Anuar Mohamed[2], Abid Hussanan[3], Nazila Ishak[4], Norhafizah Md Sarif[5], Mohd Zuki Salleh[6*]

Applied & Industrial Mathematics Research Group,
Faculty of Industrial Sciences & Technology,
Universiti Malaysia Pahang, Malaysia.
hasmawani@shahputra.edu.my[1], baa_khy@yahoo.com[2], abidhussnain_utm@yahoo.com[3], nazilaishak@gmail.com[4], fairyiza@gmail.com[5], zukikuj@yahoo.com[6*]

Abstract—the stagnation flow and heat transfer of a Williamson viscous fluid towards a stretching surface with slip conditions and viscous dissipation is studied. With the help of similarity transformation, the governing equations are converted to nonlinear ordinary differential equations and then solved numerically by Runge-Kutta-Fehlberg (RKF) technique. Numerical results for the local Nusselt number and skin friction coefficient as well as the temperature and velocity field are elucidated through tables and graphs. The influence of Prandtl number, stretching parameter, non-Newtonion Williamson fluid parameter, Eckert number, thermal and velocity slip parameter on the flow and heat transfer characteristics are analyzed and discussed.

Keywords—Numerical solution; Slip Condition; Stagnation point flow; stretching sheet; non-Newtonian Williamson Fluid; Viscous Dissipation.

1. INTRODUCTION

The study of non-Newtonion fluids has attracted attention for many researchers' nowdays. In fact, it has many theoretical and technical applications both in industries and engineering processes. In addition, the boundary layers flow of non-Newtonion fluids has been used in the aerodynamic extrusion of plastic sheets, glass fiber, paper production, manufacturing of polymer sheets (Nadeem et al. [1]), oil recovering and food processing (Das et al. [2]). In view of their difference with Newtonion fluids, many models of non-Newtonion fluilds have been proposed such as the Jefferey fluid (Das et al. [2]), the second-grade fluid (Nadeem et al. [3]), the Casson fluid (Ramesh and Devakar [4]), the micropolar fluid (Borrelli et al. [5]), the Williamson fluid (Nadeem et al. [6]) and so much more. In this studied the Williamson viscous fluids are considered.

Williamson [7] was the first who discussed the flow of pseudoplastic materials and developed a model equation to illustrate the flow of pseudoplastic fluids. Next, Nadeem et al. [6] investigated the flow of a Williamson fluid over a stretching sheet. The homotopy analysis is being used to solve the nonlinear differential equation. After that, Khan et al. [8] investigated the boundary layer flow of Williamson fluid with chemically reactive species using scaling transformation and homotopy analysis method. It is found that the Williamson model of non-newtonian fluid is very much similar to the blood and almost completely describes of blood flow. The homotopy analysis is considered to solve analytical solution of the governing problem. In addition, Nadeem and Hussain [9]considered the flow and heat transfer analysis of Williamson nanofluid. The governing non-linear equations are solving analytically using homotopy analysis method.

The flow near the stagnation point refers to the vertical flow hit perpendicularly the horizontal surface which generated the stagnation line. The external velocity is employed in the negative *y*-direction perpendicular to the flat plate while the stretching velocity is applied along the horizontal surface (Wang [10];Salleh et al. [11]). According to Wang [10], the utmost pressure, utmost heat transfer and the utmost rates of mass deposition are encountered by the stagnation region. Problem associated with boundary layer flows on stagnation point and stretching surface has fascinated many researchers.

Hiemenz [12] was the first who proposed the problem involved stagnation point and managed to solve exact value for Navier-Stokes equations. Next, Chao and Jeng [13] investigated the unsteady stagnation point heat transfer. After that, Mahapatra and Gupta [14] was also investigated the stagnation point flow with heat transfer and solved using finite difference method known as Thomas algorithm.Then, Nazar et al. [15] extended the same problem of Mahapatra and Gupta [14] by consider micropolar fluid. The Keller-box method is being used to solve the system of nonlinear ordinary differential equations and as a matter of fact, increadible concurrence with Mahapatra and Gupta [14] for resultant Newtonian fluid. In addition, Ishak et al. [16] considered the mixed convection stagnation-point flow towards a vertical stretching sheet. The transformed ordinary differential equations are solving numerically by using Keller-box method. After that, unsteady linear viscouselastic fluid model over a stretching/shrinking sheet in the region of stagnation point flows was analyzed by Khan et al. [17] and solved by using homotopy analysis method. Then, Makinde et al. [18] studied the buoyancy effects on MHD stagnation point flow and heat transfer of a nanofluid past a convectively heated stretching/shrinking sheet. It is found that both the skin friction coefficient and the local Sherwood number decrease while the local Nusselt number increases with increasing intensity of buoyancy force. In addition, MHD stagnation point flow and heat transfer due to nanofluid towards a stretching sheet was discussed by Ibrahim et al. [19]. The governing non-linear boundary-layer equations were solving numerically by using Runge-Kutta fourth order method with shooting technique. This paper found that the heat transfer rate at the surface increases with the magnetic parameter when the free stream velocity exceeds the stretching velocity. Furthermore, Nandy and Mahapatra [20] investigated effects of slip and heat generation/absorption on MHD stagnation flow of nanofluid past a stretching/shrinking surface with convective boundary boundary conditions. Moreover, flow and heat transfer of nanofluids at a stagnation point flow over a stetching/shrinking surface in porous medium with thermal radiation was analyzed by Pal et al. [21]. This paper found that skin friction coefficient increases for both stretching/shrinking sheet with increases in volume fraction of the nanoparticles.

Meanwhile in considering the viscous dissipation effects, from literature study it is found that Gebhart [22] is the first person investigated viscous dissipation in free convection flow. After that, the viscous dissipation effects on unsteady free convective flow over a vertical porous plate was analyzed by Soundalgekar [23]. Then, Vajravelu and Hadjinicolaou [24] studied the viscous dissipation effects on the flow and heat transfer over a stretching sheet. In addition, the heat transfer in microtubes with viscous dissipation discussed by Tunc and Bayazitoglu [25]. Then, Nield et al. [26] investigated viscous dissipation effects on force convection through parallel channel in a porous medium with uniform temperature and axial conduction. Recently, Cortell [27] investigated the effects of viscous dissipation and radiation on thermal boundary layer over a nonlinearly stretching sheet. Moreover, MHD effects on heat transfer over stretching sheet embedded in porous medium with variable viscosity, viscous dissipation and heat source/sink was investigated by Dessie and Kishan [28]. After that, Gnaneswara Reddy et al. [29] was analyzed the effects of viscous dissipation and heat source on unsteady MHD flow over a stretching sheet. The governing non-linear partial differential equations are solved by applying Keller Box method. Then, Pal and Mandal [30] investigated mixed convection-radiation on stagnation point flow of nanofluids over a stretching/shrinking sheet in a porous medium with heat generation and viscous dissipation. These papers conclude the important note that addition of nanoparticles into base fluid produced an increase in the skin firction coefficient.

Besides of others' investigations, the flow field obeys the no slip conditions. It is known that no slip conditions state that a solid body will not be having any velocity relative to the body at the control surface of the moving fluid in contact (Prabhakara and Deshpande [31]). According to Bhattacharyya et al. [32], the no slip assumptions is not applicable for all cases of fluid flow. It is due to some situations where the no slip conditions may be replaced with partial or slip condition. Meanwhile, slip conditions is the action when fluid at plate surface will have none zero velocity. Martin and Boyd [33] analyzed the momentum and heat transfer in a laminar boundary layer with slip flow. Futhermore, Aman et al. [34] studied the slip effects in mixed convection boundary layer flow on vertical surface near the stagnation-point while Sahoo [35] considered partial slip on stretching sheet embedded in non-Newtonian fluid. Moreover, Raisi et al. [36] investigated forced convection laminar flow of nanofluid through a microchannel in the presence as well as in the absence of slip effects. Recently, Mahmoud and Waheed [37] as well as Nandy and Mahapatra [20] observed the slip and heat generation/absorption effects on MHD stagnation flow past a stretching surface in nanofluid and micropolar fluid, respectively. In addition, Ibrahim and Shankar [38] was studied MHD boundary layer flow and heat transfer of a nanofluid past a permeable stretching sheet with velocity, thermal and solutal slip boundary conditions. Next, heat transfer analysis due to an unstedy stretching/shrinking cylinder with partial slip condition and suction was investigated by Abbas et al. [39]. Moreover, Das et al. [2] was analyzed the radiative flow of MHD Jeffery fluid past a stretching sheet with surface slip and melting heat transfer. Then, stagnation point flow of a hydromagnetic viscous fluid over stretching/shrinking sheet with generalized slip condition in the presence of homogeneous-heterogeneous reactions was studied by Abbas et al. [40]. The governing partial differential equations are solve

numerically by using shooting method. The result of this paper show that for the shrinking sheet, dual solutions exist in the certain range involved parameters, while for stretching sheet, the solutions are unique.

The aim of present work is to investigate the flow and heat transfer analysis of Williamson viscous fluid on the stagnation point past a stretching surface in the presence of viscous dissipation and slip conditions. A similar transformation is first used to transform the governing non linear partial differential equations into an ordinary differential equations system before RKF method is used numerically. Present problem has not been studied before, and then the results reported here are new.

2. MATHEMATICAL FORMULATIONS

Consider the steady two-dimensional flow of a Williamson fluid over a stretching plate as shown in Figure 1. The external and stretching velocities are $u_e(x) = ax$ and $u_w(x) = c\,x$, where *a* and *b* are constants. It is further assumed that the plate is subjected obey the slip conditions. The boundary layer equations are (Salleh et al. [41]):

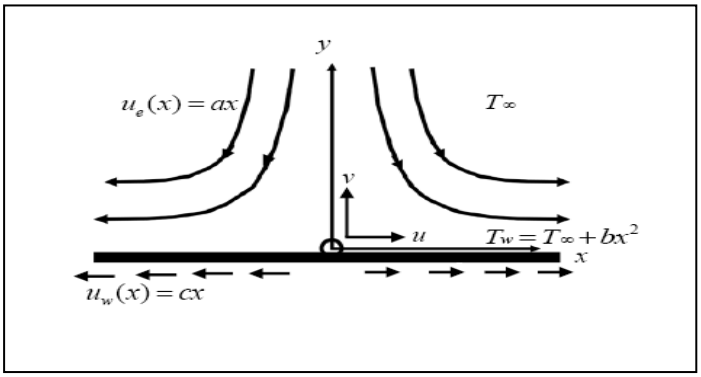

FIGURE 1: Physical model of the coordinate system

$$\frac{\partial u}{\partial x} + \frac{\partial v}{\partial y} = 0 \tag{1}$$

$$u\frac{\partial u}{\partial x} + v\frac{\partial u}{\partial y} = u_e\frac{du_e}{dx} + \nu\frac{\partial^2 u}{\partial y^2} + \sqrt{2}\;\nu\Gamma\frac{\partial u}{\partial y}\frac{\partial^2 u}{\partial y^2} \tag{2}$$

$$u\frac{\partial T}{\partial x} + v\frac{\partial T}{\partial y} = \frac{k}{\rho C_p}\frac{\partial^2 T}{\partial y^2} + \frac{\mu}{\rho C_p}\left(\frac{\partial u}{\partial y}\right)^2 \tag{3}$$

corresponds to the following conditions

$$u = u_w(x) + \gamma^*\mu\frac{\partial u}{\partial y}, \quad v = 0, \quad T = T_w + \beta^*\frac{\partial T}{\partial y} \quad \text{at } y = 0$$
$$u \to u_e(x), \quad T \to T_\infty \quad \text{as} \quad y \to \infty \tag{4}$$

where *u* and *v* are the velocity in the *x* and *y* axises, $T_w(x) = T_\infty + bx^2$ is the wall temperature, ν is the kinematic viscosity, *T* is the fluid temperature, γ^* is the dimensional velocity slip parameter, β^* is the dimensional thermal slip parameter, *k* is the thermal conductivity, ρ is the fluid density, C_p is the specific heat, Γ is the time constant and μ is the dynamic viscosity.
Now, we introduce the following similarity variables (Salleh et al. [42]):

$$\eta = \left(\frac{c}{\nu}\right)^{1/2} y, \qquad \psi = (c\nu)^{1/2} x f(n), \qquad \theta(\eta) = \frac{T - T_\infty}{T_w - T_\infty}, \tag{5}$$

where ψ is the stream function

$$u = \frac{\partial \psi}{\partial y} \text{ and } v = -\frac{\partial \psi}{\partial x},$$

By using above functions, Equation (1) is identically satisfies.

Thus, we obtain

$$u = cxf'(\eta), \qquad v = -(c\nu)^{1/2} f(\eta) \tag{6}$$

here prime represents differentiation with respect to η. By using (5) and (6), equations (2) and (3), becomes:

$$f''' + ff'' + \varepsilon^2 - f'^2 + \lambda f''f''' = 0 \tag{7}$$

$$\theta'' - \Pr\left[2f'\theta - f\theta'\right] + \Pr\ Ec\ f''^2 = 0 \tag{8}$$

where $\Pr = \frac{\nu \rho C_p}{k}$ is the Prandtl number, $Ec = \frac{c^2}{c_p b}$ is the Eckert number which represent the viscous dissipation parameter, $\lambda = x\Gamma\sqrt{\frac{2c^3}{\nu}}$ is the non newtonion Williamson parameter and $\varepsilon = \frac{a}{c}$ is the stretching parameter .The boundary conditions (4) become

$$f(0) = 0, \quad f'(0) = 1 + \gamma f''(0), \quad \theta(0) = 1 + \beta\theta'(0) \tag{9}$$

$$f'(\eta) \to \varepsilon, \quad \theta(\eta) \to 0 \qquad \text{as} \quad \eta \to \infty \tag{10}$$

Further, $\gamma = \gamma^* \rho (c\nu)^{1/2}$ and $\beta = \beta^* \left(\frac{c}{\nu}\right)^{1/2}$ is the dimensionless velocity and thermal slip parameter, respectively. It is noticed that $\beta = 0$ is when the wall temperature remains constant (CWT).

The skin friction coefficient C_f and the local Nusselt number Nu are given as

$$C_f = \frac{\tau_w}{\rho u_w^2}, \quad Nu = \frac{-x}{T_w - T_\infty} \left.\frac{\partial T}{\partial y}\right|_{y=0} \tag{11}$$

The surface shear stress τ_w is defined as

$$\tau_w = \mu \frac{\partial u}{\partial y}\left[1 + \Gamma\sqrt{\frac{1}{2}\frac{\partial u}{\partial y}}\right] \tag{12}$$

Using the similarity variables in (5) give

$$C_f\, \mathrm{Re}_x^{1/2} = f''(0) + \frac{\lambda}{2}\left(f''(0)\right)^2, \qquad Nu_x\, \mathrm{Re}_x^{-1/2} = -\theta'(0) \tag{13}$$

where $\mathrm{Re}_x = \frac{cx^2}{\nu}$ is the local Reynolds number.

3. RESULTS AND DISCUSSION

Equations (7) and (8) with corresponding boundary conditions (9) and (10) are solved numerically with the help of Runge-Kutta-Fehlberg method. To study the flow behavior, we considered different parameters, namely the Prandtl number $\Pr$, the dimensionless velocity slip parameter γ, the dimensionless thermal slip parameter β, the stretching parameter ε, the non-Newtonion Williamson parameter λ and the Eckert number Ec. In order to validate the efficiency of the method used, the comparison values of reduced skin friction coeffienct $f''(0)$ has been made.

Tables 1 and 2 show the comparison result with the previously published results for different values of λ and ε**.** It is found that the results present in both tables are in a good agreement, therefore we are confident with the results accuracy in this problem.

Table 3 presents the various values of the non-Newtonion Williamson parameter λ. The results found that as λ increases the $-\theta'(0)$ decreases as well as $f''(0)$. The trend of decreasing in $-\theta'(0)$ and $f''(0)$ is just the values declining slowly.

Table 4 presents the various values of the dimensionless thermal slip parameter β. The results found that as β increases the $\theta(0)$ decreases as well as $-\theta(0)$. The trend of decreasing in $-\theta'(0)$ and $f''(0)$ is just the values declining slowly.

Table 5 presents the various values of the dimensionless velocity slip parameter γ. The results found that as γ increases the $\theta(0)$ decreases meanwhile the $-\theta(0)$ increases. The trend of decreasing in $-\theta'(0)$ is just the values declining slowly and for incresing in $-\theta(0)$ the values ascending slowly.

Figure 2 points the temperature profiles for various values of Pr. Since the value of Pr rises, it is found that the value of the wall temperature and the thickness of the thermal boundary layer dropped. Physically, its means when we, the thermal diffusivity decreased as Pr increases and these phenomena lead to the decrease of the energy ability and which results the thermal boundary layer decreases.

Figure 3 demonstrates the temperature profiles for various values of ε. The data found in Figure 3 were similar to Figure 2, where as ε rises, the value of the wall temperature and the thickness of thermal boundary declines.

Table 1. Comparison of the present results to those obtained in previous works when $\Pr = 1$, $Ec = 0$, $\gamma = 0$ and $\beta = 0$

ε	**Mahapatra and Gupta [14]**	**Nazar et al. [43]**	**Ishak et al. [16]**	**Present**
	$f''(0)$	$f''(0)$	$f''(0)$	$f''(0)$
0.1	- 0.9694	- 0.9694	- 0.9694	- 0.96938
0.2	- 0.9181	- 0.9181	- 0.9181	- 0.91810
0.5	- 0.6673	- 0.6673	- 0.6673	- 0.66726
2	2.0175	2.0176	2.0175	2.017502
3	4.7293	4.7296	4.7294	4.729282

Table 2. Comparison of the present results to those obtained in previous works when $\Pr = 3$, $Ec = 0$, $\gamma = 0$, $\varepsilon = 0$ and $\beta = 0$

λ	**Nadeem et al. [6]**	**Nadeem and Hussain [9]**	**Present**
	$f''(0)$	$f''(0)$	$f''(0)$
0.1	-1.03446	-	-1.034527
0.2	-	-1.076	-1.076289

Table 3. Values of $-\theta'(0)$ and $f''(0)$ for the various values of λ when $\Pr = 1$, $\beta = 1$, $\varepsilon = 3$, $Ec = 1$ and $\gamma = 1$.

λ	$-\theta'(0)$	$f''(0)$
0.1	0.63632	1.43531
3	0.61729	1.18022
5	0.61588	1.09802
7	0.61585	1.03969
9	0.61628	0.99467

Table 4. Values of $\theta(0)$ and $-\theta'(0)$ for the various values of β when $\Pr = 1$, $\lambda = 1$, $\varepsilon = 3$, $Ec = 1$ and $\gamma = 1$.

β	$\theta(0)$	$-\theta'(0)$
0.7	0.47236	0.75377
3	0.17279	0.27574
9	0.06509	0.10388
13	0.04599	0.07339
20	0.03038	0.04848

Table 5. Values of $\theta(0)$ and $-\theta'(0)$ for the various values of γ when $\Pr = 1$, $\beta = 1$, $\varepsilon = 3$, $Ec = 1$ and $\lambda = 1$.

γ	$\theta(0)$	$-\theta'(0)$
0.7	0.43632	0.56368
3	0.28625	0.71375
9	0.26925	0.73075
13	0.26776	0.73224
20	0.26683	0.73317

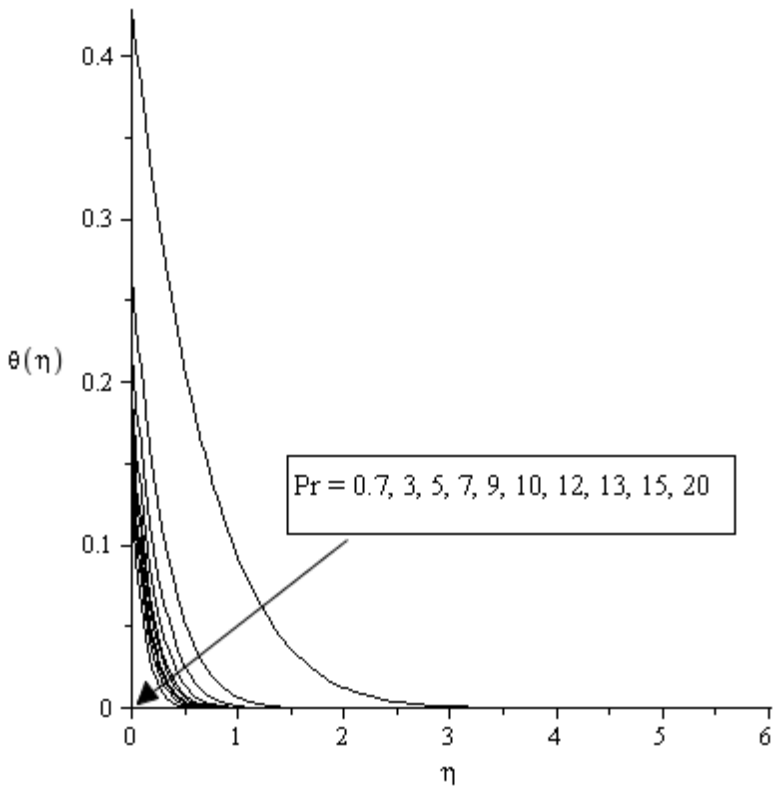

FIGURE 2: Temperature $\theta(\eta)$ for various values of Pr when $\beta = 1$, $\varepsilon = 1$, $Ec = 1$, $\lambda = 1$ and $\gamma = 1$

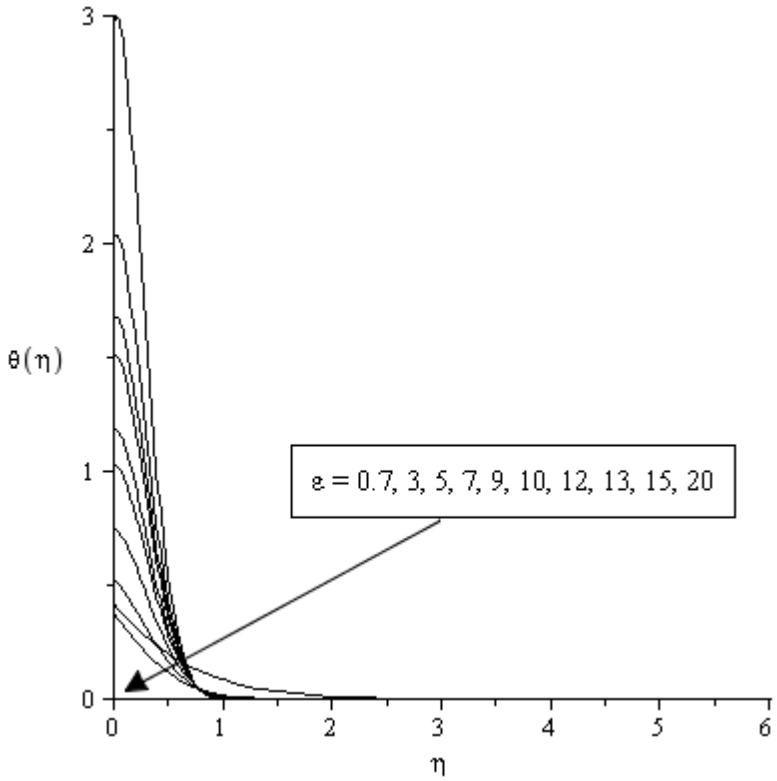

FIGURE 3: Temperature $\theta(\eta)$ for various values of ε when $\beta = 1$, $\Pr = 1$, $Ec = 1$, $\lambda = 1$ and $\gamma = 1$

Figure 4 presented the temperature distribution for different values of Ec. Note, $Ec = 0$ refers to the case when viscous dissipation is not present. From figure, the temperature profiles increases as Ec increases. This is because of the fact that due to large viscous resistance there is more accumulation of heat energy in the fluid particles near the boundary. Also it is noticed that Ec only give a small effect for boundary layer thickness.

Next, Figures 5 and 6 present the temperature profile for various values of β $\beta$and γ, respectively. Similar trends occurred between this both figure where the temperature profiles and boundary layer thickness θ decrease as β or γ increases. Physically we can conclude that the present of both velocity and thermal slip parameter reduced the temperature and the boundary layer thickness.

Figure 7 present the velocity profile and skin friction coefficient for several of the velocity slip parameter γ respectively. From Figure 7, it is found that the velocity gradient decreases as γ increases.

Figure 8 present the temperature profile for various values of non-Newtonion Williamson parameter λ respectively. From this figure, it is found that the temperature profiles and boundary layer thickness increases as λ decreases.

Figure 9 present the velocity profile and skin friction coefficient for various values of non-Newtonion Williamson parameter λ respectively. From this figure, it is found that the velocity gradient increases as well as λ decreases.

Figure 10 and 11 illustrate the wall temperature and heat transfer coefficient with λ for various values of Ec. Note, only positive values of λ will discuss in this area. From this figure, it can be seen that no solution can be obtained as λ past its critical value. Further, it is understand the values of λ must be small because to high values of λ will effect enough to stop the heat transfer process. In addition, the increase of Ec results to the increase of wall temperature and heat transfer coefficient as well as increase the range of λ for which the solutions exists. It shown that when $Ec = 1$ the physical

acceptable solution occur until $\lambda_{c1} = 28.69035$ meanwhile the results for Ec increase to $Ec = 7$, λ stops at the critical point $\lambda_{c1} = 51.03014$.

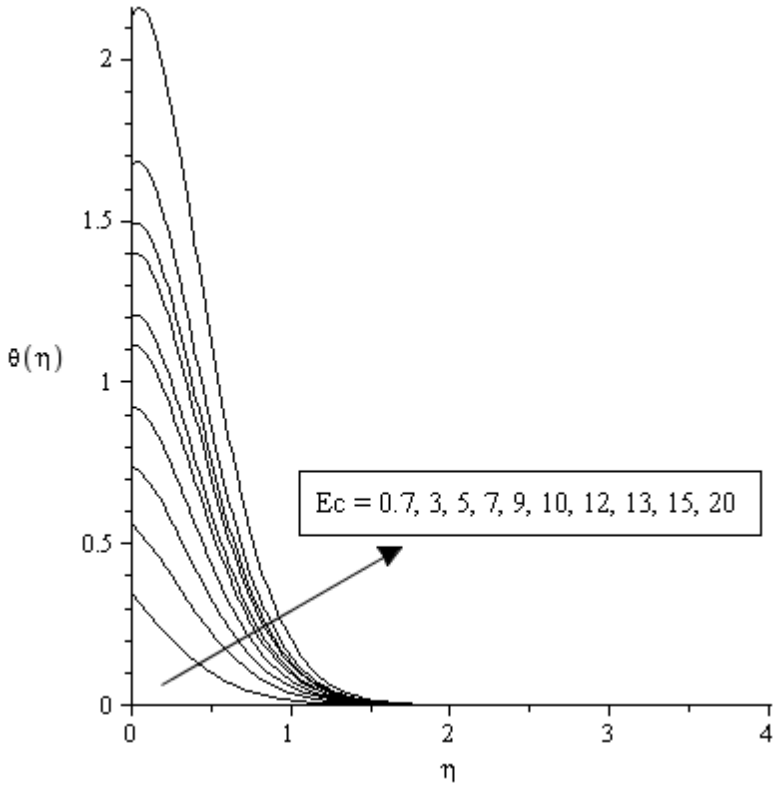

FIGURE 4: Temperature $\theta(\eta)$ for various values of Ec when $\beta = 1$, $\Pr = 1$, $\varepsilon = 3$, $\lambda = 1$ and $\gamma = 1$

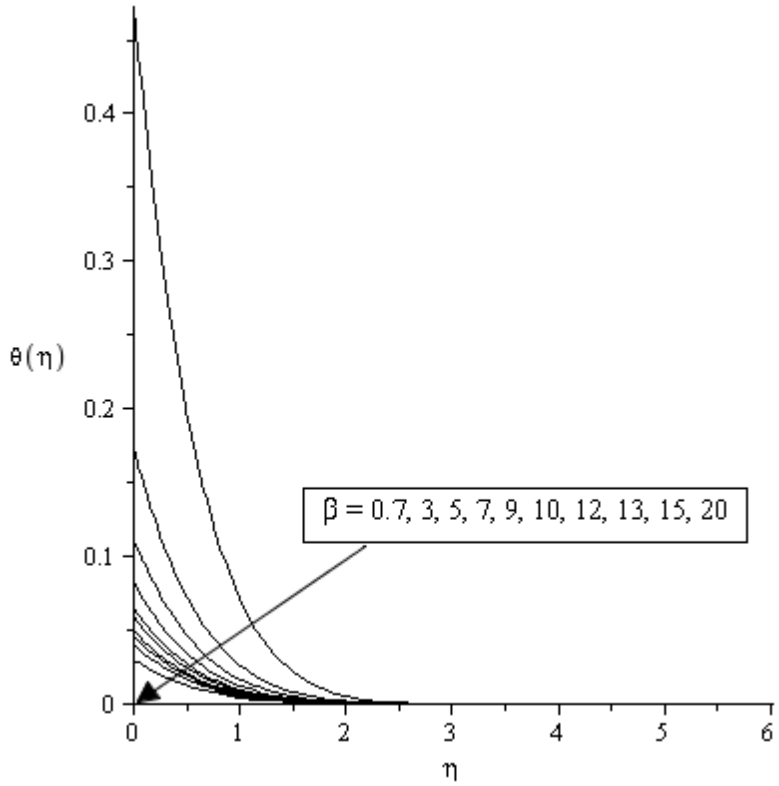

FIGURE 5: Temperature $\theta(\eta)$ for various values of β when $\varepsilon = 1$, $\Pr = 1$, $Ec = 1$, $\lambda = 1$ and $\gamma = 1$

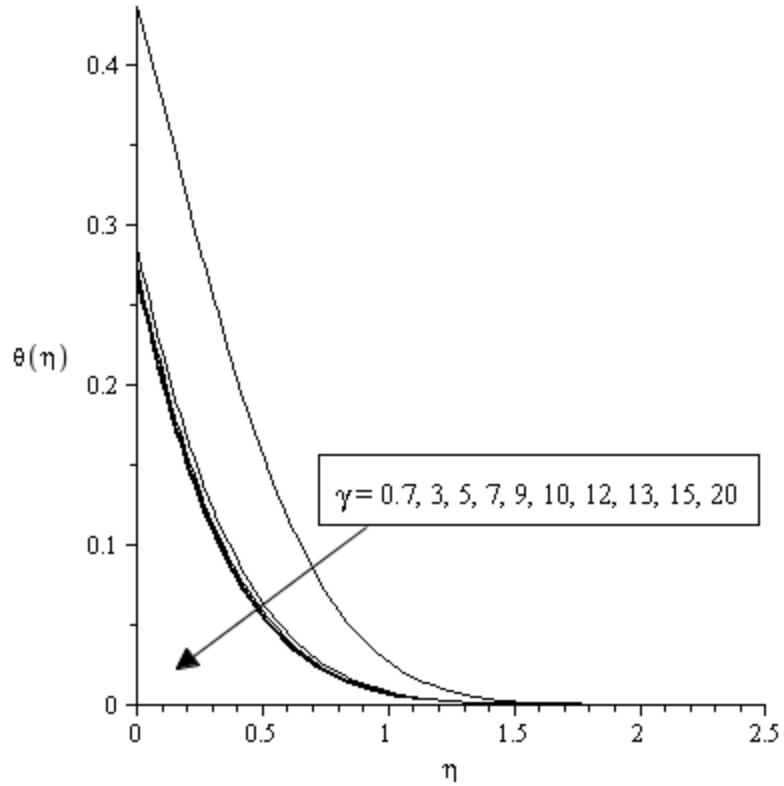

FIGURE 6: Temperature $\theta(\eta)$ for various values of γ when $\beta = 1$, $\Pr = 1$, $Ec = 1$, $\lambda = 1$ and $\varepsilon = 3$

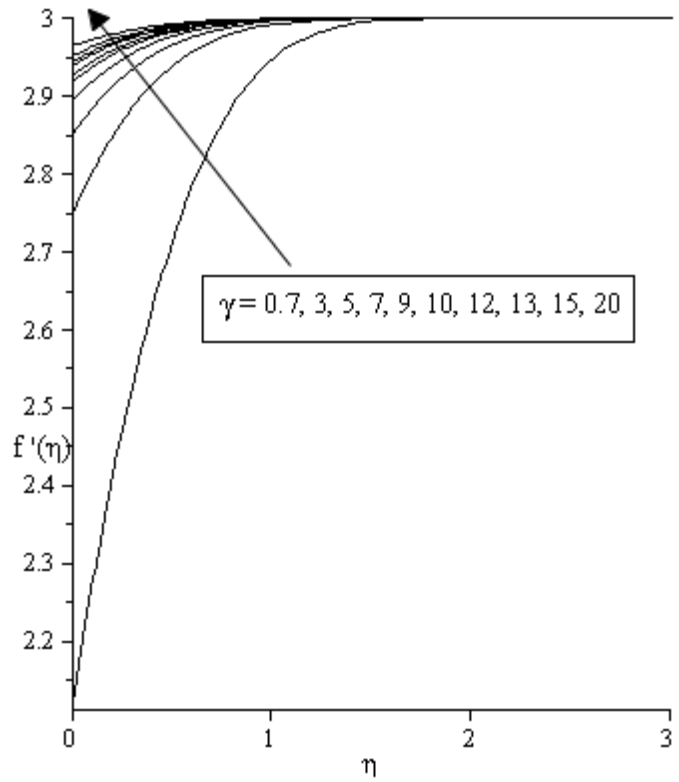

FIGURE 7: Velocity profiles $f'(\eta)$ for various values of γ when $\beta = 1$, $\Pr = 1$, $Ec = 1$, $\lambda = 1$ and $\varepsilon = 3$

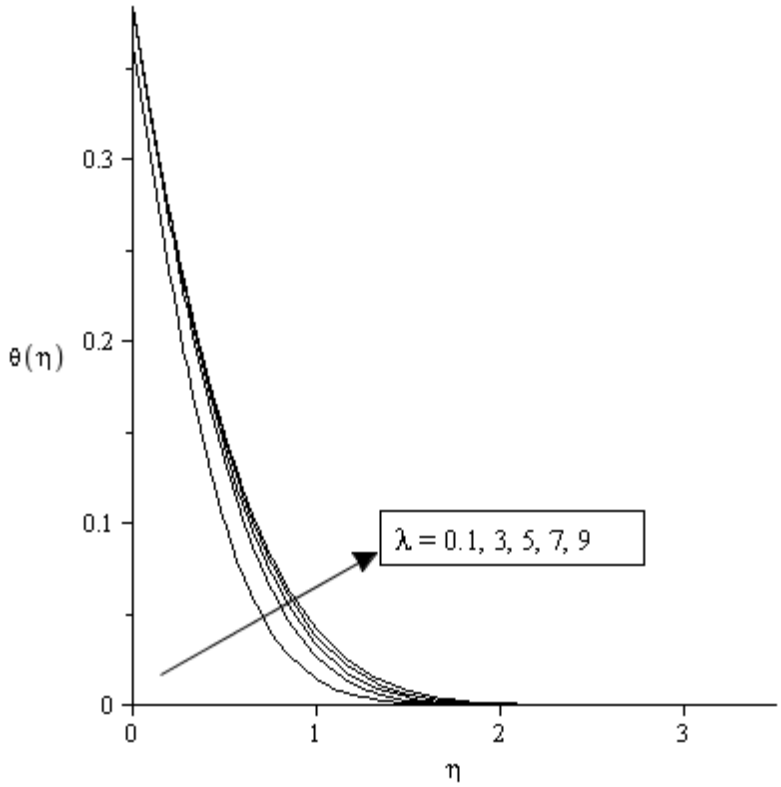

FIGURE 8: Temperature $\theta(\eta)$ for various values of λ when $\beta = 1$, $\mathrm{Pr} = 1$, $Ec = 1$, $\gamma = 1$ and $\varepsilon = 3$

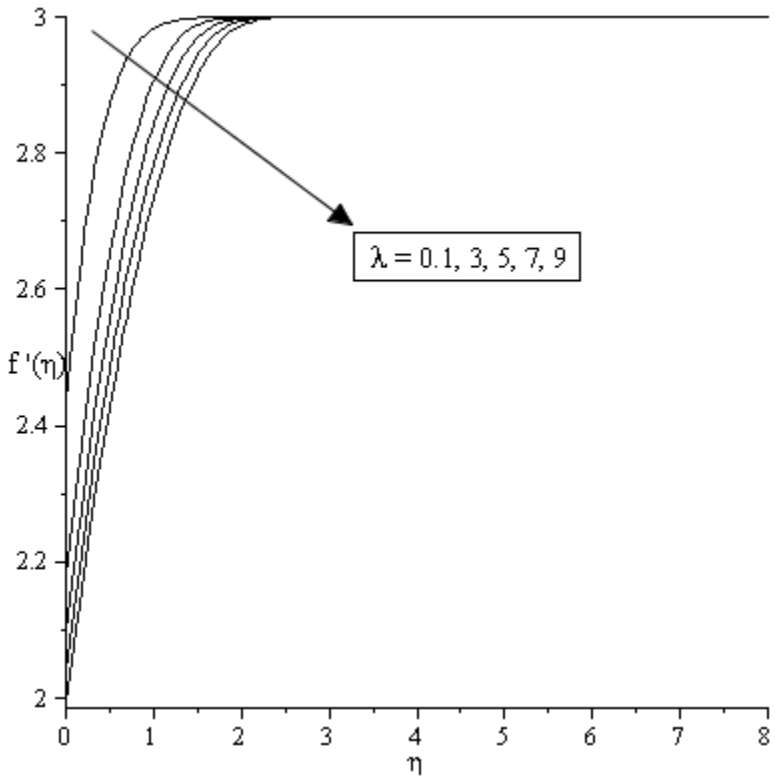

FIGURE 9: Velocity profiles $f'(\eta)$ for various values of λ when $\beta = 1$, $\mathrm{Pr} = 1$, $Ec = 1$, $\gamma = 1$ and $\varepsilon = 3$

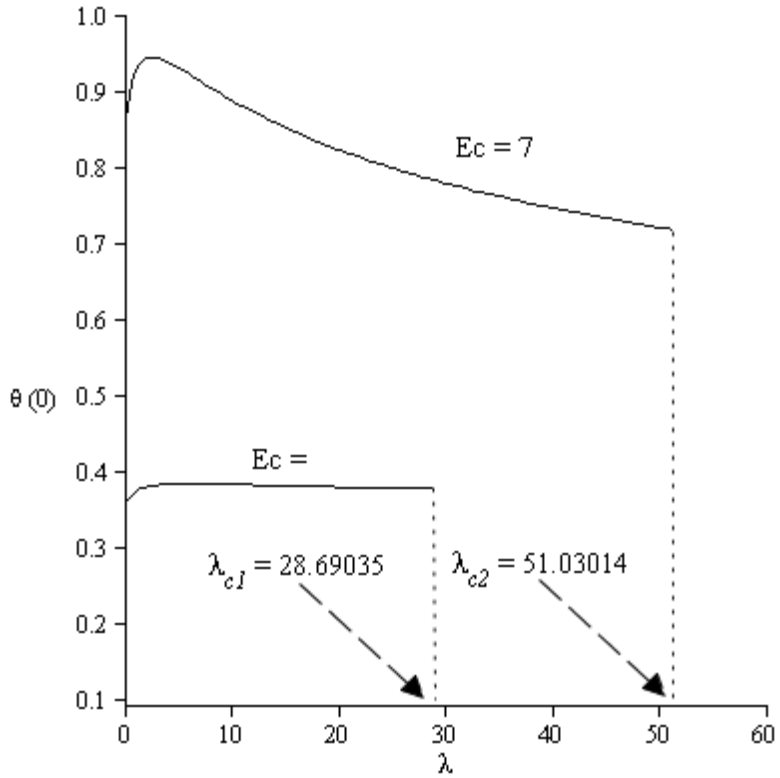

FIGURE 10: Distribution of wall temperature $\theta(\eta)$ against with λ for various values of Ec when $\Pr = 1, \beta = 1, \varepsilon = 3$ and $\gamma = 1$

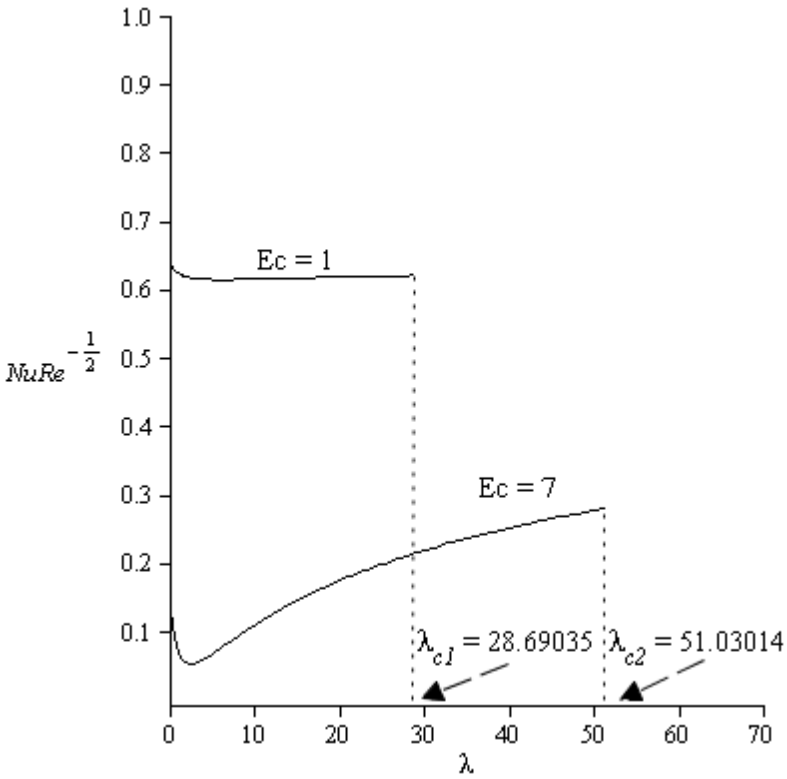

FIGURE 11: Distribution of heat transfer coefficient $Nu\,\mathrm{Re}^{-\frac{1}{2}}$ against with λ for various values of Ec when $\Pr = 1, \beta = 1, \varepsilon = 3,$ and $\gamma = 1$

4. CONCLUSION

In this paper, the stagnation flow and heat transfer of a Williamson viscous fluid towards a stretching surface with slip conditions and viscous dissipation is numerically studied. The values of the reduced Nusselt number and the skin friction coefficient as well as the temperatura and velocity profiles are affected by Prandtl number Pr, velocity slip parameter γ, stretching parameter ε, thermal slip parameter β, Eckert number Ec and non-Newtonion Williamson viscous fluid parameter. As a conclusion, the increases of Prandtl number, stretching parameter, dimensionless thermal and velocity slip parameter result to the decreasing in the wall temperature and also thermal boundary layer thickness. Meanwhile, the presence of viscous dissipation and non-Newtonion Williamson viscous fluid parameter results to increases of the wall temperature.

In addition, the increase of Ec results to the increase of wall temperature and heat transfer coefficient as well as increase the range of λ for which the solutions exists.

Next, it is suggested that, in the presence of velocity slip parameter is decreased by the skin friction coefficient but not for non-Newtonion Williamson viscous fluid parameter the velocity gradient is increases while the Prandtl number, the stretching parameter, the thermal slip parameter and Eckert number gives no effect on the skin friction coefficient.

ACKNOWLEDGMENT

The authors thank University Malaysia Pahang for the financial supports RDU140111 (FRGS) and RDU150101 (FRGS)

REFERENCES

[1] Nadeem, S., Hussain, A., Malik, M. & Hayat, T. (2009). Series solutions for the stagnation flow of a second-grade fluid over a shrinking sheet. Applied Mathematics and Mechanics, 30(10), 1255-1262.

[2] Das, K., Acharya, N. & Kundu, P. K. (2015). Radiative flow of MHD Jeffrey fluid past a stretching sheet with surface slip and melting heat transfer. Alexandria Engineering Journal,

[3] Nadeem, S., Hussain, A. & Vajravelu, K. (2010). Effects of heat transfer on the stagnation flow of a third-order fluid over a shrinking sheet. Zeitschrift für Naturforschung A, 65(11), 969-994.

[4] Ramesh, K. & Devakar, M. (2015). Some analytical solutions for flows of Casson fluid with slip boundary conditions. Ain Shams Engineering Journal, 6(3), 967-975.

[5] Borrelli, A., Giantesio, G. & Patria, M. C. (2012). MHD oblique stagnation-point flow of a micropolar fluid. Applied Mathematical Modelling, 36(9), 3949-3970.

[6] Nadeem, S., Hussain, S. & Lee, C. (2013). Flow of a Williamson fluid over a stretching sheet. Brazilian Journal of Chemical Engineering, 30(3), 619-625.

[7] Williamson, R. V. (1929). The flow of pseudoplastic materials. Industrial & Engineering Chemistry, 21(11), 1108-1111.

[8] Khan, N. A., Khan, S. & Riaz, F. (2014). Boundary Layer Flow of Williamson Fluid with Chemically Reactive Species using Scaling Transformation and Homotopy Analysis Method. Mathematical Sciences Letters, 3(3), 199.

[9] Nadeem, S. & Hussain, S. (2014). Flow and heat transfer analysis of Williamson nanofluid. Applied Nanoscience, 4(8), 1005-1012.

[10] Wang, C. Y. (2008). Stagnation flow towards a shrinking sheet. International Journal of Non-Linear Mechanics, 43(5), 377-382.

[11] Salleh, M. Z., Mohamed, N., Khairuddin, R., Khasi'ie, N. S. & Nazar, R. 2009. Numerical Study of Free Convection Boundary Layer Flow on a Vertical Surface with Prescribed Wall Temperature, Heat Flux and Newtonian Heating Using Shooting Method. Proceedings of the International Conference on Software Engineering and Computer Systems (ICSECS'09). UMP, Kuantan**:** hlm. 94-98.

[12] Hiemenz, K. (1911). DIe Grenzschicht an einem in den gleichformigen Flussigkeitsstrom eingetauchten ger-aden Kreiszylinder. Dingley's Polytechnic Journal, 32, 321-410.

[13] Chao, B. T. & Jeng, D. R. (1965). Unsteady stagnation point heat transfer. Journal of Heat Transfer 87, 221-230.

[14] Mahapatra, T. R. & Gupta, A. S. (2002). Heat transfer in stagnation-point flow towards a stretching sheet. Heat and Mass transfer, 38(6), 517-521.

[15] Nazar, R., Amin, N., Filip, D. & Pop, I. (2004). Stagnation point flow of a micropolar fluid towards a stretching sheet. International Journal of Non-Linear Mechanics, 39(7), 1227-1235.

[16] Ishak, A., Nazar, R. & Pop, I. (2006). Mixed convection boundary layers in the stagnation-point flow toward a stretching vertical sheet. Meccanica, 41(5), 509-518.
[17] Khan, Y., Hussain, A. & Faraz, N. (2012). Unsteady linear viscoelastic fluid model over a stretching/shrinking sheet in the region of stagnation point flows. Scientia Iranica, 19(6), 1541-1549.
[18] Makinde, O. D., Khan, W. A. & Khan, Z. H. (2013). Buoyancy effects on MHD stagnation point flow and heat transfer of a nanofluid past a convectively heated stretching/shrinking sheet. International Journal of Heat and Mass Transfer, 62, 526-533.
[19] Ibrahim, W., Shankar, B. & Nandeppanavar, M. M. (2013). MHD stagnation point flow and heat transfer due to nanofluid towards a stretching sheet. International Journal of Heat and Mass Transfer, 56(1–2), 1-9.
[20] Nandy, S. K. & Mahapatra, T. R. (2013). Effects of slip and heat generation/absorption on MHD stagnation flow of nanofluid past a stretching/shrinking surface with convective boundary conditions. International Journal of Heat and Mass Transfer, 64, 1091-1100.
[21] Pal, D., Mandal, G. & Vajravelu, K. (2014). Flow and heat transfer of nanofluids at a stagnation point flow over a stretching/shrinking surface in a porous medium with thermal radiation. Applied Mathematics and Computation, 238, 208-224.
[22] Gebhart, B. (1962). Effects of viscous dissipation in natural convection. Journal of Fluid Mechanics, 14(02), 225-232.
[23] Soundalgekar, V. M. (1972). Viscous dissipation effects on unsteady free convective flow past an infinite, vertical porous plate with constant suction. International Journal of Heat and Mass Transfer, 15(6), 1253-1261.
[24] Vajravelu, K. & Hadjinicolaou, A. (1993). Heat transfer in a viscous fluid over a stretching sheet with viscous dissipation and internal heat generation. International Communications in Heat and Mass Transfer, 20(3), 417-430.
[25] Tunc, G. & Bayazitoglu, Y. (2001). Heat transfer in microtubes with viscous dissipation. International Journal of Heat and Mass Transfer, 44(13), 2395-2403.
[26] Nield, D., Kuznetsov, A. & Xiong, M. (2003). Thermally developing forced convection in a porous medium: parallel plate channel with walls at uniform temperature, with axial conduction and viscous dissipation effects. International Journal of Heat and Mass Transfer, 46(4), 643-651.
[27] Cortell, R. (2008). Effects of viscous dissipation and radiation on the thermal boundary layer over a nonlinearly stretching sheet. Physics Letters A, 372(5), 631-636.
[28] Dessie, H. & Kishan, N. (2014). MHD effects on heat transfer over stretching sheet embedded in porous medium with variable viscosity, viscous dissipation and heat source/sink. Ain Shams Engineering Journal, 5(3), 967-977.
[29] Gnaneswara Reddy, M., Padma, P. & Shankar, B. (2015). Effects of viscous dissipation and heat source on unsteady MHD flow over a stretching sheet. Ain Shams Engineering Journal, 6(4), 1195-1201.
[30] Pal, D. & Mandal, G. (2015). Mixed convection–radiation on stagnation-point flow of nanofluids over a stretching/shrinking sheet in a porous medium with heat generation and viscous dissipation. Journal of Petroleum Science and Engineering, 126, 16-25.
[31] Prabhakara, S. & Deshpande, M. (2004). The no-slip boundary condition in fluid mechanics. Resonance, 9(5), 61-71.
[32] Bhattacharyya, K., Mukhopadhyay, S. & Layek, G. C. (2011). Slip effects on boundary layer stagnation-point flow and heat transfer towards a shrinking sheet. International Journal of Heat and Mass Transfer, 54(1–3), 308-313.
[33] Martin, M. J. & Boyd, I. D. (2006). Momentum and heat transfer in a laminar boundary layer with slip flow. Journal of thermophysics and heat transfer, 20(4), 710-719.
[34] Aman, F., Ishak, A. & Pop, I. (2011). Mixed convection boundary layer flow near stagnation-point on vertical surface with slip. Applied Mathematics and Mechanics, 32(12), 1599-1606.
[35] Sahoo, B. (2010a). Flow and heat transfer of a non-Newtonian fluid past a stretching sheet with partial slip. Communications in Nonlinear Science and Numerical Simulation, 15(3), 602-615.
[36] Raisi, A., Ghasemi, B. & Aminossadati, S. (2011). A numerical study on the forced convection of laminar nanofluid in a microchannel with both slip and no-slip conditions. Numerical Heat Transfer, Part A: Applications, 59(2), 114-129.
[37] Mahmoud, M. A. A. & Waheed, S. E. (2012). MHD flow and heat transfer of a micropolar fluid over a stretching surface with heat generation (absorption) and slip velocity. Journal of the Egyptian Mathematical Society, 20(1), 20-27.
[38] Ibrahim, W. & Shankar, B. (2013). MHD boundary layer flow and heat transfer of a nanofluid past a permeable stretching sheet with velocity, thermal and solutal slip boundary conditions. Computers & Fluids, 75, 1-10.
[39] Abbas, Z., Rasool, S. & Rashidi, M. (2015). Heat transfer analysis due to an unsteady stretching/shrinking cylinder with partial slip condition and suction. Ain Shams Engineering Journal,
[40] Abbas, Z., Sheikh, M. & Pop, I. (2015). Stagnation-point flow of a hydromagnetic viscous fluid over stretching/shrinking sheet with generalized slip condition in the presence of homogeneous–heterogeneous reactions. Journal of the Taiwan Institute of Chemical Engineers, 55, 69-75.
[41] Salleh, M. Z., Nazar, R. & Pop, I. (2009). Forced Convection Boundary Layer Flow At a Forward Stagnation Point with Newtonian Heating. Chemical Engineering Communications, 196, 987-996.

[42] Salleh, M. Z., Nazar, R. & Pop, I. (2010). Boundary layer flow and heat transfer over a stretching sheet with Newtonian heating. Journal of the Taiwan Institute of Chemical Engineers, 41(6), 651-655.

[43] Nazar, R., Amin, N., Filip, D. & Pop, I. (2004). Unsteady boundary layer flow in the region of the stagnation point on a stretching sheet. International journal of engineering science, 42(11), 1241-1253.